ISSN 0915-633X

NATIONAL INSTITUTE FOR FUSION SCIENCE

Electrophoresis of Charge Inverted Macroion Complex: Molecular Dynamics Study

M. Tanaka and A. Yu. Grosberg

(Received - June 26, 2001)

NIFS-706 July 2001

RESEARCH REPORT
NIFS Series

TOKI, JAPAN

Electrophoresis of Charge Inverted Macroion Complex: Molecular Dynamics Study

Motohiko Tanaka[1], and A Yu. Grosberg[2]
[1] *National Institute for Fusion Science, Toki 509-5292, Japan*
[2] *Department of Physics, University of Minnesota, Minneapolis, MN 55455*

Charge inversion and mobility of a macroion in the presence of multivalent counterions and monovalent coions under an external electric field are studied by molecular dynamics simulations. The hydrodynamic interactions are treated with the explicit use of neutral-particle solvent In a weak electric field, a complex of the macroion with condensed counterions and coions drifts along the electric field, in the direction proving the inversion of the charge sign. The electrophoretically determined net charge of the complex is smaller than that of the peak of radial charge distribution, indicating that many co-ions along with counter-ions are involved in the drift. Very large electric field disrupts charge inversion stripping the adsorbed counterions off the macroion, which happens at the order of macroion unscreened electric field consistently with the correlation theory of charge inversion.

Keywords: Overscreening, multivalent counterions, mobility, hydrodynamic interactions, critical electric field.

I. Introduction

The concept of electrostatic screening is well known to every physicist for three quarters of a century since Debye and Hückel [1]. In recent years, it was understood that screening by strongly charged ions may lead to such counterintuitive phenomena as attraction between like charged macroions [2,3] and inversion of macroion charge [4]. As regards charge inversion, it was intensely discussed in the experimental literature on colloids well over fifty years ago [5], but its understanding is just forming (see recent review article [6] and references therein). In particular, in our companion paper [7], we reported observation of charge inversion with a molecular dynamics experiment.

What is charge inversion ? Consider a strongly charged macroion (see, e.g., Fig.1); to be specific, suppose its charge is negative. It is surrounded predominantly by positive counterions and, if the counterion charge Z is large, their number turns out greater than necessary to neutralize the macroion. Thus, the macroion with the Z-ions form a positive complex. This is charge inversion. Of course, a question immediately arises: the positively charge inverted complex will now be surrounded predominantly by negative ions, and ... we seem to be arriving at a logical loop. In fact, as it was emphasized in Ref. [8], only those ions should be counted as comprising a complex that are bound with energies in excess of k_BT. However appealing, this criteria is not easy to implement.

Meanwhile, experimentally finding out the charge *sign* is straightforward - it is determined by the direction of the electrophoretic drift under an externally applied electric field. This is precisely the procedure used long ago to observe charge reversal for macroscopic coacervate droplets [5], and it can be used now to observe charges of much smaller ions [9–11]. We therefore undertake in this paper to examine the external field behavior of a charge inverted complex. Our goal is three fold. First, we would like to confirm that the direction of electrophoretic drift is determined by the sign of the inverted charge. Second, we want to check how the speed of the weak field drift depends on the inverted charge and the Stokesian friction. Third, it is interesting to see how large is the field that disrupts a charge inverted complex and pulls macroion in the direction determined by its bare charge.

The difficulty to simulate electrophoresis is in the importance of hydrodynamic interactions. Indeed, naively one may try to use the Langevin equation, assuming that every ion in the system is subject to Stokesian friction force $-6\pi\eta av$ (in standard notations) and some white noise random force balanced with friction through the fluctuation-dissipation theorem. This approach, however simple, is hardly justifiable. Indeed, if two balls stick together, neither their corresponding friction nor random kick forces add to each other. One way to resolve this problem would be to incorporate hydrodynamic interaction forces using the Oseen tensor [12]. This is not easy to implement in numerical simulations, because it produces complicated spatial correlations between random forces. We, therefore, opt to address the problem by a brutto force approach, explicitly adopting neutral solvent particles in molecular dynamics simulation.

II. Simulation Method and Parameters

We consider the following model, assuming a, e, and m the units of length, charge and mass, respectively. Spherical macroion with hard core radius R_0 between $3a$ and $6a$ and negative charge Q_0 between $-15e$ and $-60e$ is surrounded by some N^+ counterions of positive charge Ze each and $N^- \approx 300$ coions of charge $(-e)$ each. The system is overall neutral, $Q_0 + N^+Ze - N^-e = 0$, which determines N^+ for every Z. Counterions and coions are spherical, with hard core radius a. There are also some N_* neutral particles; they are spheres of hard core radius $a/2$ each. The mass of macroion is $M = 200m$, masses of co- and counter-ions are m, and masses of neutral particles are $m/2$. The system is confined in the simulation domain - a cube of the size $L = 32a$, with periodic bound-

ary conditions in all three directions.

Calculation of the Coulomb forces under such conditions involves the charge sum in the first Brillouin zone and their infinite mirror images (the Ewald sum [13]). The sum is calculated with the use of the PPPM algorithm [14]. We use $(32)^3$ space meshes for the calculation of the reciprocal space contributions to the Coulomb force, with the Ewald parameter $\alpha \approx 0.262$ and the real-space cutoff $r_{cut} = R_i + 10a$, where R_i is the radius of the i-th ion. Uniform electric field E is applied in the x-direction.

The number of neutral particles is about 8000; it is chosen such that there is volume $(32a/21)^3$ per each one of them inside the simulation domain excluding the place occupied by the macroion and other ions. On top of Coulomb forces, all particles interact through the repulsive Lennard-Jones potential $\phi_{LJ} = 4\epsilon[(\sigma/r_{ij})^{12} - (\sigma/r_{ij})^6]$ for $r_{ij} = |\mathbf{r}_i - \mathbf{r}_j| \leq 2^{1/6}\sigma$ ($\sigma = 2a$) and $\phi_{LJ} = -\epsilon$ otherwise. We choose $\epsilon = k_BT = e^2/5a$.

To start molecular dynamics simulation, we prepare initial state by randomly positioning all ions and neutral particles in the simulation domain and choosing their initial velocities from the Maxwell distribution corresponding to some temperature T_{initial}. We integrate Newton equations of motion with the use of the leapfrog method [15], which is equivalent to the Verlet algorithm. In the absence of the electric field $E = 0$, our system is closed, and its energy is conserved. After the initial transient phase, the distribution of velocities becomes again Maxwellian, suggesting equilibrium sampling of the microcanonical ensemble. This new Maxwell distribution corresponds to the temperature T which is somewhat higher than T_{initial}, because of the release of potential energy due to screening - local balancing of charges. We adjust T_{initial} such that $k_BT = \epsilon$. This sets ϵ as the unique relevant scale of energy and, accordingly, we put $\tau = a\sqrt{m/\epsilon}$ as the unit of time. We use $\Delta t = 0.01\tau$ as the integration time step. The simulation runs are executed up to 1000τ. Given the value of ϵ chosen above, our temperature corresponds to $e^2/ak_BT = 5$.

When an external electric field is present, it performs some work on the system (although it should be emphasized that there is no momentum transfer into the system, because the system is overall charge neutral). Corresponding energy, which is Joule heat, is transferred to background neutral particles through collisions with accelerated ions. To simulate the electrophoretic bath being kept at a constant temperature, we re-scale velocities of all neutral particles once in every 100τ returning temperature to T. This procedure maintains temperature stable to within 5%.

III. Simulation Results

The results of our simulations are summarized in Figs.1-5. Figure 1 is the bird's-eye view of all the ions (a) and the vicinity of the macroion (b). Counterions are shown in light blue, and coions in dark blue. In this figure, macroion charge is $Q_0 = -30e$, its radius is $R_0 = 3a$, counterion valence is $Z = 3$, and the electric field is $E = 0.3\epsilon/ea$. It is seen that the macroion is predominantly covered by counterions. This is the same situation as the one observed in the absence of electric field in our previous work [7]. As in the no field case, the radially integrated charge has a sharp positive peak at the distance about a from the macroion surface. Of course, this peak is due to positive counterions adsorbed on the macroion surface. The value of peak charge under the conditions of Fig.1 is $Q_{\text{peak}} \approx 1.6|Q_0|$. Is this value the right characteristics of the charge inversion ? In other words, do these counterions drift with macroion in electrophoresis, and, at the same time, do any coions drift with this complex ?

Figure 2 demonstrates the time history of the "peak" charge (a) and macroion drift speed (b) for the parameters of Fig.1. There is a short transient phase during which a charge inverted complex is formed through adsorption of counterions to the macroion and condensation of coions on the counterions. This process is reflected in a rather quick rise in Q_{peak}, as is shown in Fig.2(a). At the time $t = 10\tau$, we "switch" external electric field on. After the transient phase, we observe a drift of the macroion in the *positive direction*, along the applied field. The fact that drift velocity is positive, as Fig.2(b) indicates, for the negative macroion bare charge ($Q_0 < 0$), is the direct manifestation that counterions are so strongly bound that they pull the macroion with them.

Note that the drift velocity shown in Fig.2(b) is small compared to v_0 - thermal velocity of neutral particles: $\langle V_x \rangle \sim 0.05v_0$. Under this condition, exchange of momentum between macroion and neutral particles is slow, and requires many collisions (compare consideration of the similar system in Ref. [16]). Therefore, in terms of hydrodynamics, we are in the linear regime, and should expect average drift speed to be given by the force balance $Q^*E - \nu V_x \approx 0$, where Q^* is the effective (net) charge of the complex and ν is the hydrodynamic friction coefficient.

We measured this friction coefficient in an independent simulation, by observing an exponential decay of the macroion velocity starting from $0.5v_0$ for the case without the electric field. We found $\nu \approx 7.2m/\tau$ for the *neutral* ball of the radius $R_0 = 3a$. In fact, relevant friction may be larger because macroion drifts as a complex with counter- and co-ions which contribute to its effective size. Measurement of friction coefficient for an artificial particle in which co-and counterions are firmly attached to the macroion in a typical configuration produced during our simulations yields $\nu \approx 14.0m/\tau$.

Using the latter value of the friction coefficient, we find effective charge $Q^* \approx \nu \langle V_x \rangle / E \approx 4.7e$ for the case of Fig.1. In other words, this result means charge inver-

sion ratio of $Q^*/|Q_0| \approx 0.16$. This is roughly a quarter of the value corresponding to the peak of charge distribution, $(Q_{\rm peak} - |Q_0|)/|Q_0| \approx 0.6$. This discrepancy tells us about the important contribution of coions which are adsorbed on counterions and thus cup the charge inversion.

Figure 2 shows also significant temporal fluctuations of the drift speed. Inspection shows that the fluctuations are larger than what one would expect due to random kicks of neutral particles. In fact, these fluctuations indicate that the counterions are not permanently attached to the macroion and coions not to counterions, but that they are being swamped, or replaced from time to time.

The electric field dependence of the average macroion drift speed $V_{\rm drift}$ is shown in Fig.3. Let us first discuss the small field, linear drift regime.

At small fields, $V_{\rm drift}$ increases linearly with the field. This regime corresponds to regular Ohm's law. In this regime a macroion drifts together with its ionic atmosphere as an unperturbed complex, with the net charge of the complex insensitive to the electric field. In other words, electric field is not strong enough to affect binding of counterions with the macroion. Small field regime is characterized with the mobility, $\mu = \langle V_x \rangle / E$. Assuming friction coefficient is a constant, mobility is directly proportional to the net charge of the complex.

The dependence of the macroion mobility μ on the valence of counterions Z in Fig.4 is physically interesting and also important for application purposes. To begin with, note that mobility is *negative* for monovalent counterions at $Z = 1$. This means that charge inversion does not happen in the solution of regular monovalent salt, which is consistent both with our previous molecular dynamics study [7] and with the understanding [6] that charge inversion is entirely due to correlations between strongly charged ions. At $Z \geq 2$, charge inversion does take place, as manifested by *positive* mobility. The mobility first increases with the valence, but saturates at $Z > 4$. This can be understood by noticing that at large Z, monovalent negative ions start to condense on the positive Z-ions, effectively reducing the charge of the latter. This is consistent with our previous observations [7] showing massive adsorption of monovalent coions on Z-ions for high valences.

Figure 5 shows that the mobility of the macroion first increases linearly with the macroion bare charge and becomes nearly independent for large macroion charges, where the radius R_0 is kept constant. The linear regime is again consistent with our previous observations [7], and the saturation regime is attributed to neutralization of the complex by condensed coions.

Let us now return to Fig.3 and discuss the regime that is nonlinear in the applied field. As the figure indicates, at large electric field the charge inverting shell around macroion is destroyed. Furthermore, the figure itself leads us to the estimate of the critical field at which this happens. The field in the abscissa in Fig.3 is normalized to $|Q_0|/R_0^2$. Therefore, the figure indicates that the critical value of $ER_0^2/|Q_0|$ is independent of the macroion size, yielding the critical field

$$E_c \approx 0.35|Q_0|/R_0^2 \,. \qquad (1)$$

This result is very interesting. Indeed, $|Q_0|/R_0^2$ is the electric field created on the macroion surface by the macroion bare charge. Why does the critical field not scale with net charge of the complex instead of bare charge of the macroion ? The reason is due to correlations between screening ions. We noted while discussing Fig.2 that the counterions on the macroion surface are being replaced from time to time. Consider, therefore, how one Z-ion can depart from the macroion surface. Since this ion is surrounded by a correlation hole on the surface, its departure will require work against the unscreened bare electric field of the macroion surface as long as its distance from the surface is smaller than the distance between adsorbed Z-ions. Therefore, when the external field becomes competitive to this unscreened field of the correlation hole, departure from the surface becomes essentially barrier-free, and at such field the charge inverted complex is no longer stable.

The critical electric field in realistic situations is estimated to be quite large. For the parameters $R_0 \approx 20\mathring{A}$, $Q_0 \approx 30e$, the critical electric field becomes as large as $E_c \approx 0.35 Q_0/\varepsilon R_0^2 \approx 50 V/\mu m$, where we took into account the dielectric constant of water, $\varepsilon \approx 80$ [18]. Therefore, in practice the applied electric field is not expected to disrupt charge inversion.

IV. Summary

In this paper, we directly proved the occurrence of charge inversion and measured the net charge of the macroion complex by electrophoresis of a macroion immersed in electrolyte solvent. The weak electric field did not disrupt the charge inverted complex, but pulled it in the direction determined by the inverted charge. Although academic, the larger fields regime in which electrophoresis is strongly nonlinear was interesting because the field stripped screening counter-ions off the macroion. Consistent with the correlation theory, this happened at the order of *unscreened* macroion field.

Acknowledgments

The authors are grateful to Professor B.Shklovskii and Dr.T.Nguyen for discussions of charge inversion phenomenon. One of the authors (M.T.) thanks Professor K.Kremer and Dr.C.Holm for collaboration on the PPPM algorithm for periodic Coulomb systems, the work of which was done during his stay at the Max-Planck Institut für Polymerforschung (Mainz, fall 1999) under the support of the Max-Planck Society.

References

1. P. Debye and E. Hückel, *Phys.Zeitsch., 24*, 185 (1923).

2. T.Squires and M.Brenner, *Phys.Rev.Lett., 85*, 4976 (2000).

3. I. Rouzina and V. A. Bloomfield, *J. Phys. Chem., 100*, 9977 (1996).

4. B.I.Shklovskii, *Phys. Rev. E, 60*, 5802 (1999).

5. H.G. Bungenberg de Jong, in *Colloid Science*, vol.2 (edited by H.R. Kruyt, Elsevier, p.259-330 (1949)).

6. A.Yu. Grosberg. T.T. Nguyen, and B.I. Shklovskii, *preprint cond-mat/0105140.*

7. M.Tanaka and A.Yu Grosberg, *J. Chem. Phys., 115, July 1* (2001).

8. T.T.Nguyen, A.Yu Grosberg and B.I. Shklovskii, *Phys. Rev. Lett., 85*, 1568 (2000).

9. J.Xia and P. L. Dubin, *Macromolecular complexes in Chemistry and Biology* (edited by P.L.Dubin et al., Springer-Verlag, Berlin, 1994).

10. H.M. Evans, A. Ahmad, T. Pfohl, A. Martin and C.R. Safinya, *Bull. APS, 46*, 391 (2001).

11. H.W. Walker and S.B. Grant, *Colloids and Surfaces A, 119*, 229 (1996).

12. L.D. Landau and E.M. Lifshitz, *Theoretical Physics, vol. 6, Fluid Mechanics* (Butterworth-Heinemann, 1990).

13. P.P.Ewald, *Ann.Physik, 64*, 253 (1921).

14. J.W.Eastwood and R.W.Hockney, *J. Comput. Phys., 16*, 342 (1974).

15. D.Frenkel and B.Smit, *Understanding Molecular Simulation* (Academic Press, 1996)

16. E.M. Lifshitz and L.P. Pitaevskii, *Theoretical Physics, vol. 10, Physical Kinetics*, Chap.2 (Butterworth-Heinemann, 1981).

17. T.T.Nguyen, private communication.

18. Although critical field is large, it gives only small energy to the electric dipole of a water molecule, $d \approx 2 \times 10^{-18}$esu $\cdot$ cm: $E_c d/k_B T \sim 0.07 \ll 1$.

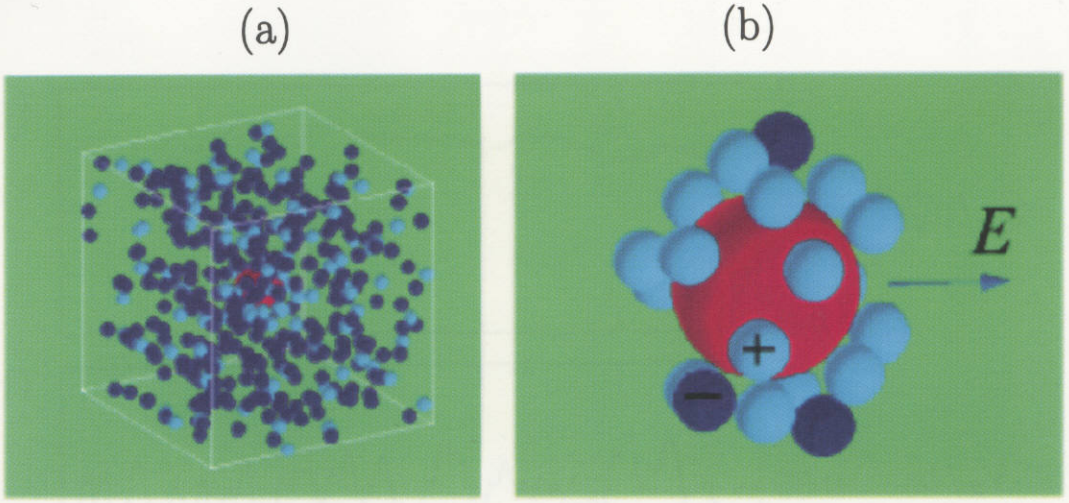

Figure 1. The bird's-eye view of (a) all the ions in the simulation domain, and (b) the screening ion atmosphere within $3a$ from the macroion surface. Macroion with charge $Q_0 = -30e$ and radius $R_0 = 3a$ is a large sphere in the middle; counterions ($Z = 3$) and monovalent coions are shown by light and dark blue spheres, respectively. The arrow to the right shows the direction of the electric field (x-axis), with $E = 0.3\epsilon/ea$.

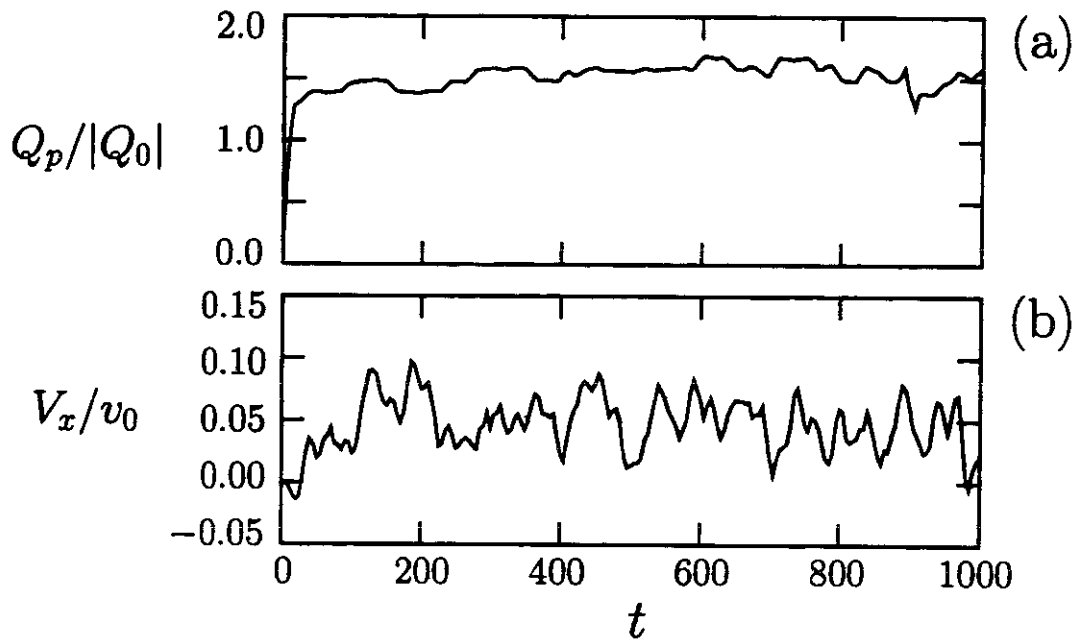

Figure 2. The time history of (a) the "peak" charge Q_p, and (b) macroion speed V_x normalized by thermal velocity of neutral particles v_0. The macroion complex drifts positively along the external electric field for $E > 0$, which directly proves the inversion of the charge sign.

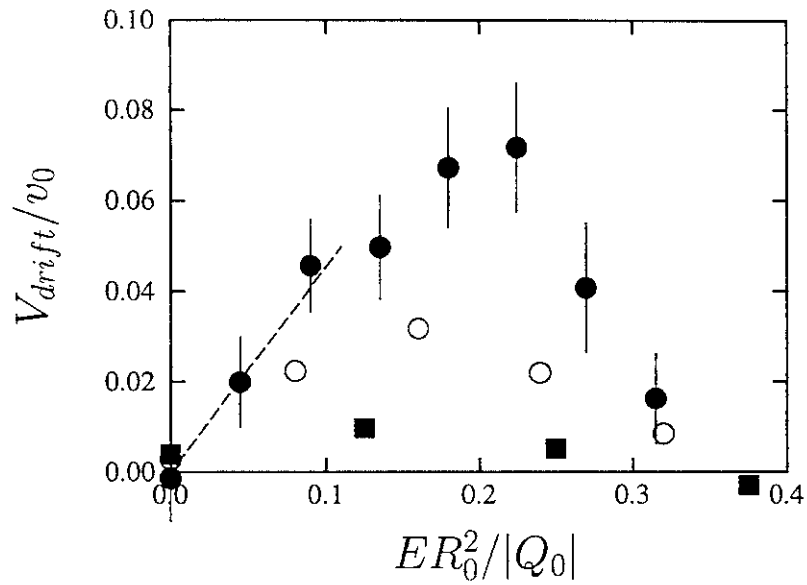

Figure 3. Dependence of the macroion drift speed $V_{\rm drift}$ on the external electric field E for the macroion of three different radii, $R_0 = 3a$ (filled circle), $R_0 = 4a$ (open circle) and $R_0 = 5a$ (square). Other parameters are: macroion charge $Q_0 = -30e$, and the valence of counterions $Z = 3$.

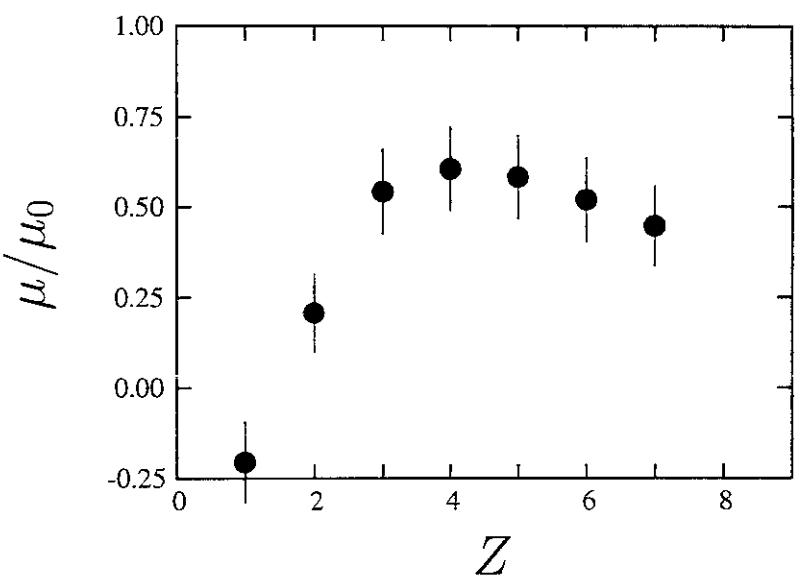

Figure 4. Dependence of mobility of the macroion μ on the valence of counterions Z, where $\mu_0 = v_0/(|Q_0|/R_0^2)$. The parameters are $R_0 = 3a$, $Q_0 = -30e$, and $E = 0.3\epsilon/ae$.

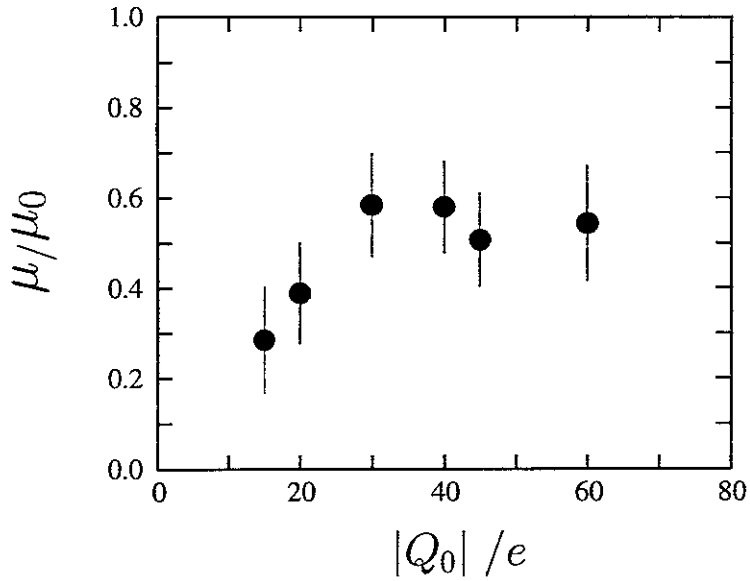

Figure 5. Dependence of the macroion mobility μ on the macroion charge Q_0, where $\mu_0 = v_0/(|Q_0^{(0)}|/R_0^2)$, and the parameters are $Q_0^{(0)} = -30e$, $R_0 = 3a$, valence $Z = 3$, $E = 0.3\epsilon/ae$, and $e^2/ak_BT = 5$.

Recent Issues of NIFS Series

NIFS-680 A Yoshizawa, N Yokoi, S Nisizima, S-I Itoh and K Itoh
Variational Approach to a Turbulent Swirling Pipe Flow with the Aid of Helicity Feb 2001

NIFS-681 Alexander A Shishkin
Estafette of Drift Resonances, Stochasticity and Control of Particle Motion in a Toroidal Magnetic Trap Feb 2001

NIFS-682 H Momota and G H Miley
Virtual Cathode in a Spherical Inertial Electrostatic Confinement Device Feb 2001

NIFS-683 K Saito, R Kumazawa, T Mutoh, T Seki, T Watari, Y Torii, D A Hartmann, Y Zhao, A Fukuyama, F Shimpo, G Nomura, M Yokota, M Sasao, M Isobe, M Osakabe, T Ozaki, K Narihara, Y Nagayama, S Inagaki, K Itoh, S Morita, A V Krasilnikov, K Ohkubo, M Sato, S Kubo, T Shimozuma, H Idei, Y Yoshimura, O Kaneko, Y Takeiri, Y Oka, K Tsumori, K Ikeda, A Komori, H Yamada, H Funaba, K Y Watanabe, S Sakakibara, M Shoji, R Sakamoto, J Miyazawa, K Tanaka, B J Peterson, N Ashikawa, S Murakami, T Minami, S Ohakachi, S Yamamoto, S Kado, H Sasao, H Suzuki, K Kawahata, P deVries, M Emoto, H Nakanishi, T Kobuchi, N Inoue, N Ohyabu, Y Nakamura, S Masuzaki, S Muto, K Sato, T Morisaki, M Yokoyama, T Watanabe, M Goto, I Yamada, K Ida, T Tokuzawa, , N Noda, S Yamaguchi, K. Akaishi, A Sagara, K Toi, K Nishimura, K Yamazaki, S Sudo, Y Hamada, O Motojima, M Fujiwara,
Ion and Electron Heating in ICRF Heating Experiments on LHD Mar 2001

NIFS-684 S Kida and S Goto,
Line Statistics Stretching Rate of Passive Lines in Turbulence Mar 2001

NIFS-685 R Tanaka, T Nakamura and T Yabe,
Exactly Conservative Semi-Lagrangian Scheme (CIP-CSL) in One-Dimension Mar 2001

NIFS-686 S. Toda and K Itoh,
Analysis of Structure and Transition of Radial Electric Field in Helical Systems Mar 2001

NIFS-687 T Kuroda and H Sugama,
Effects of Multiple-Helicity Fields on Ion Temperature Gradient Modes Apr 2001

NIFS-688 M Tanaka,
The Origins of Electrical Resistivity in Magnetic Reconnection Studies by 2D and 3D Macro Particle Simulations Apr 2001

NIFS-689 A Maluckov, N Nakajima, M Okamoto, S Murakami and R Kanno,
Statistical Properties of the Neoclassical Radial Diffusion in a Tokamak Equilibrium Apr 2001

NIFS-690 Y. Matsumoto, T Nagaura, Y Itoh, S-I Oikawa and T Watanabe,
LHD Type Proton-Boron Reactor and the Control of its Peripheral Potential Structure. Apr 2001

NIFS-691 A Yoshizawa, S.-I Itoh, K Itoh and N Yokoi,
Turbulence Theories and Modelling of Fluids and Plasmas· Apr 2001

NIFS-692 K Ichiguchi, T Nishimura, N Nakajima, M Okamoto, S -i. Oikawa, M. Itagaki,
Effects of Net Toroidal Current Profile on Mercier Criterion in Heliotron Plasma Apr 2001

NIFS-693 W Pei, R Horiuchi and T Sato,
Long Time Scale Evolution of Collisionless Driven Reconnection in a Two-Dimensional Open System Apr 2001

NIFS-694 L.N. Vyacheslavov, K Tanaka, K Kawahata,
CO2 Laser Diagnostics for Measurements of the Plasma Density Profile and Plasma Density Fluctuations on LHD Apr 2001

NIFS-695 T Ohkawa,
Spin Dependent Transport in Magnetically Confined Plasma May 2001

NIFS-696 M Yokoyama, K Ida, H Sanuki, K Itoh, K Narihara, K Tanaka, K Kawahata, N Ohyabu and LHD experimental group
Analysis of Radial Electric Field in LHD towards Improved Confinement: May 2001

NIFS-697 M Yokoyama, K. Itoh, S. Okamura, K Matsuoka, S. -I Itoh,
Maximum-J Capability in a Quasi-Axisymmetric Stellarator May 2001

NIFS-698 S-I. Itoh and K. Itoh,
Transition in Multiple-scale-lengths Turbulence in Plasmas May 2001

NIFS-699 K. Ohi, H. Naitou, Y Tauchi, O Fukumasa,
Bifurcation in Asymmetric Plasma Divided by a Magnetic Filter May 2001

NIFS-700 H Miura, T Hayashi and T Sato,
Nonlinear Simulation of Resistive Ballooning Modes in Large Helical Device June 2001

NIFS-701 G Kawahara and S Kida,
A Periodic Motion Embedded in Plane Couette Turbulence June 2001

NIFS-702 K Ohkubo,
Hybrid Modes in a Square Corrugated Waveguide June 2001

NIFS-703 S -I Itoh and K Itoh,
Statistical Theory and Transition in Multiple-scale-lengths Turbulence in Plasmas June 2001

NIFS-704 S Toda and K Itoh,
Theoretical Study of Structure of Electric Field in Helical Toroidal Plasmas June 2001

NIFS-705 K Itoh and S-I Itoh,
Geometry Changes Transient Transport in Plasmas June 2001

NIFS-706 M Tanaka and A Yu Grosberg
Electrophoresis of Charge Inverted Macroion Complex: Molecular Dynamics Study July 2001